M. Margalef-Rovira, M. J. Barragan, E. Sharma, P. Ferrari, E. Pistono and S. Bourdel, "An oscillation-based test technique for on-chip testing of mm-wave phase shifters," 2018 IEEE 36th VLSI Test Symposium (VTS), San Francisco, CA, 2018, pp. 1-6.
doi: 10.1109/VTS.2018.8368622

URL: http://ieeexplore.ieee.org/stamp/stamp.jsp?tp=&arnumber=8368622&isnumber=8368610

An Oscillation-Based Test technique for on-chip testing of mm-wave phase shifters

M. Margalef-Rovira†, M. J. Barragan†, E. Sharma‡, P. Ferrari†, E. Pistono‡, and S. Bourdel‡
†*Univ. Grenoble Alpes, CNRS, Grenoble INP*, TIMA F-38000 Grenoble, France*
‡ *Univ. Grenoble Alpes, CNRS, IMEP-LAHC, F-38000 Grenoble, France*
marc.margalef-rovira@univ-grenoble-alpes.fr

***Abstract*—Beam-forming techniques using phased arrays are one of the most promising solutions for the practical implementation of future high-data-rate point-to-point communication protocols. The functionality of phased arrays is based on the use of phase shifters that should provide an accurate and controllable phase difference between the different paths of the array. However, the integration of phase shifters in current nanometric technologies is prone to imperfections that may affect the intended phase shift and degrade the performance of the antenna array. This requires extensive testing and calibration and represents a bottleneck in the production line of these system. In this work, we propose a simple Oscillation-Based Test technique that may be suitable for Built-In Self-Test applications of phase shifters. The technique is demonstrated on a Reflection-Type Phase Shifter implemented in a 55 nm BiCMOS technology. Electromagnetic and electrical simulation results show the feasibility of the proposed technique.**

***Index Terms*—Phase shifters, phased arrays, Oscillation-Based Test, BIST, mm-wave integrated circuits.**

I. Introduction

The ever-increasing need of transmitting large volumes of data has led the semiconductor industry to the millimeter-wave (mm-wave) frequency band. High operating frequencies provide larger bandwidths for high-data-rate systems. In this evolution toward higher data rates, it is becoming much more difficult to improve spectral efficiency using traditional time and frequency domain techniques. A promising solution consists in taking advantage of the spatial dimension by spatially directing the antenna beam pattern.

Steering the antenna beam pattern, usually called beamforming, requires the use of a phased antenna array, or phased array. Such a system allows shaping and directing electronically the antenna beam pattern; it brings the advantages of improved Signal-to-Noise Ratio (SNR), spatial multiplexing and spatial interference cancellation. Phased arrays are used in high-end communication equipment (e.g., military communication systems) and are expanding into the consummer electronic market (e.g., car radar, high-speed communications) [1]. Indeed, beamforming has been proposed as a key enabling technology for future communication standards such as 5G cellular communications [2], [3].

A phased array is a set of multiple antennas working together as a single highly-directive antenna. In this system, the response of each individual antenna is shifted and combined in order to shape and steer the resulting radiation pattern. A phased array is composed of two main elements: the antennae and the phase shifters that interface with the front-end of the transceiver. The phase of each individual channel in the array is electrically controlled in such a way that the transmitted (or received) radio waves interfere constructively in one particular direction. This controlled phase-shift is provided by phase shifters that adjust the phase difference between the different channels in the array to combine the different signals coherently.

Even if advanced technology nodes allow the integration of phase shifters, they are prone to imperfections, such as process and mismatch variations, unintended coupling between adjacent elements, supply voltage gradients, etc., which may produce variations on the provided phase shift. Temperature drifts must be also considered. This is a key issue since small variations on a phase shift may produce large degradations in the performance of the phased array [4]–[6]. For this reason, phase shifters have to be tested and calibrated in the production line to ensure that they provide the appropriate phase shift for a correct operation. Let us notice that this does not solve the temperature drift issue. Moreover, testing and calibrating phase shifters relies on direct functional measurements using dedicated and costly mm-wave testers. In this scenario, characterizing and calibrating a complete phased array becomes a costly and time-consuming procedure that may represent a bottleneck in the production line. Developing Built-In Self-Test (BIST) strategies for phase shifters may be a promising solution to overcome these issues. BIST applications move some of the functionality of the tester to the Device Under Test (DUT) itself, in such a way that the DUT becomes self-testable, signal manipulations remain internal, and the cost of the test equipment is greatly reduced. Moreover, BIST applications may enable self-calibration during in-field operation.

In this line, a variety of test techniques have been proposed for the characterization of phased arrays and phase shifters. Thus, the works in [6]–[8] propose direct functional test techniques based on the excitation of the phased array with an external radiofrequency wave and the processing of the array response. The contact-less characterization procedures described in [7], [8] are not suitable for production line testing since they require manual adjustment and a long measurement time using dedicated test equipment. On the other hand, in [6]

*Institute of Engineering Univ. Grenoble Alpes a simplification of contact-less tests allows measuring under near-field conditions, reducing this way the physical size of the test setup.

BIST strategies for phased arrays have been also proposed in [4], [9]–[12]. In [9]–[11] a practical system-level test for phased arrays in an RF system is demonstrated: it allows characterizing and calibrating phase and amplitude inaccuracies in each individual channel of the array. The proposed test circuitry requires the integration (or re-use) of a frequency synthesizer for exciting the different channels in the array and a dedicated receiver block to extract the test information from the response signals. In the same line, the work in [4] proposes a system-level BIST and calibration circuitry for the phased array of a receiver section. BIST circuitry makes use of an LC oscillator for test stimulus generation and a simplified receiver consisting in a mixer in a homodyne configuration for test response acquisition.

The approach in [12] takes advantage of code-modulation techniques for multiplexing different test signals into orthogonal codes that are then applied to the phased array under test. An on-chip demodulator is then used to recover the test information of each individual channel.

In this work, we propose to adapt the classic Oscillation-Based Test (OBT) technique to enable self-test applications for integrated mm-wave phase shifters. To our knowledge, this is the first time that OBT is employed for the test of these mm-wave circuits. OBT, firstly introduced in [13], consists in reconfiguring the DUT into an oscillator, in such a way that the parameters of the resulting oscillation (i.e., frequency, amplitude) are directly correlated to the DUT functionality and/or performance.

Compared to previous test strategies, enabling OBT for phase shifters has a two key advantages:

1) The need of a dedicated test stimulus generator is eliminated since the DUT itself generates the test signal.
2) The interpretation of the test results is simplified since the phase shift introduced by the phase shifter is naturally encoded in the amplitude and frequency of the resulting oscillation.

In this work, it is shown that a phase shifter can be easily reconfigured as an oscillator whose frequency and amplitude are correlated to its phase shift. The proposed OBT strategy allows then to replace a complex phase measurement by simpler magnitude and frequency signatures. In addition, the proposed test strategy opens the door to a full BIST implementation due to its simplicity and low area overhead.

The rest of the paper is organized as follows. In section II, we present the proposed test approach based on OBT for the characterization of phase shifters, focusing on the Reflection-Type Phase Shifters (RTPS) as a case study. Section III describes the practical implementation of the proposed OBT architecture for a selected case study in a 55 nm BiCMOS technology and presents some relevant results obtained by electrical and electromagnetic simulations. Finally, section IV summarizes the main contributions of this work.

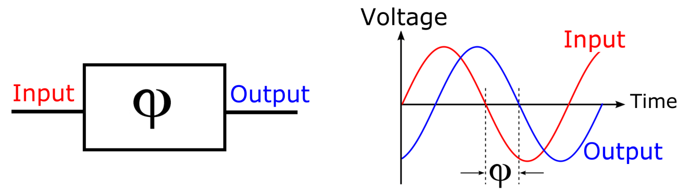

Fig. 1. Ideal phase shifter.

II. Proposed approach

As it was mentioned above, OBT was first introduced in [13] as a structural Design-for-Test approach based on reconfiguring the DUT as an oscillator. The key idea behind OBT is that any defect in the DUT would have an impact in the frequency of the resulting oscillator. This test technique has been extended to a wide variety of analog and mixed-signal applications, including the static test of Analog-to-Digital Converters [14], testing analog integrated filters [15], testing Dual-Tone Multi-Frequency receivers [16], etc.

Adapting the OBT principles to phase shifters requires to reconfigure the phase shifter itself into an oscillator in test mode, in such a way that any imperfection that may cause a deviation of the intended phase shift, would cause as well a deviation of the oscillation characteristics (i.e., frequency and/or amplitude).

An ideal phase shifter, as the one conceptually represented in Fig. 1, is a two-port device producing a controlled phase shift φ between its input and output signals without power loss at a given frequency. Several topologies of phase shifters have been presented in the literature with different phase shift control techniques. This paper focuses on electronic phase shifters based on passive components and, as a proof-of-concept case study, we will particularize the methodology to a Reflection-Type Phase Shifter (RTPS) with varactor loads. This classic phase shifter architecture, first presented in [17], offers a high precision continuous tuning of the phase shift with a good performance in terms of return and insertion loss compared to other architectures, which makes it an interesting design choice in practical mm-wave systems. It should be noted, however, that the proposed OBT technique could be applied to any other kind of electronically controlled phase shifter based on passive devices.

Without loss of generality, a RTPS with varactor loads can be electrically modeled at a particular frequency as a lossy LC-tank, as it is schematically depicted in Fig. 2, where L_{eq} and C_{eq} represent the inductive and capacitive behavior of the circuit, respectively, and R_p represents the ohmic losses of the circuit. Note that C_{eq} is a tunable capacitor, since it includes the contribution of the varactor loads.

As it is well-known, LC-tanks are lossy resonators that can be set to sustain oscillations by adding an active element that compensates the ohmic losses of the parasitic resistor [18]. This active element acts as an equivalent negative resistor and can be practically implemented using a pair of nMOS transistors in a crossed-coupled pair configuration. Figure 3

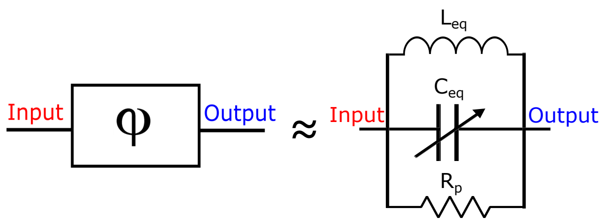

Fig. 2. Reflection-type phase shifter equivalent circuit as a lossy LC-tank. Notice that C_{eq} includes the contribution of the varactor loads of the phase shifter.

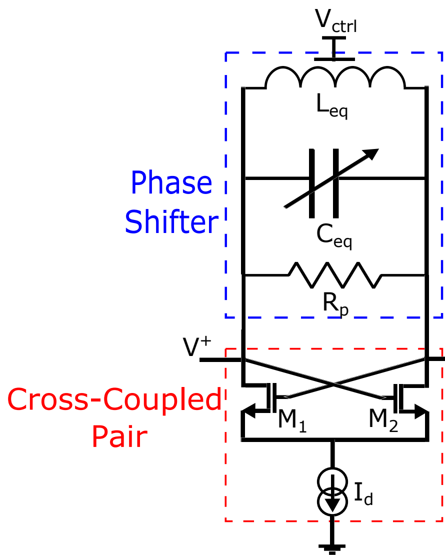

Fig. 3. Reconfiguration of a reflection-type phase shifter with varactor loads as an oscillator.

shows a conceptual block diagram of the proposed reconfiguration during the test mode, in which the phase shifter under test –represented in Fig. 3 as its equivalent lossy LC-tank– is connected to a cross-coupled pair. Note that the V_{ctrl} power supply of the resulting oscillator corresponds to the biasing voltage of the varactor loads in the RTPS. In order to produce sustained oscillations, the Barkhausen criteria has to hold. A closed-loop system as the one in Fig. 3, consisting in a lossy complex impedance $Z(j\omega_0)$ (i.e., the lossy LC tank) and a block that exhibits a gain g_m (i.e., the transconductance of the nMOS transistors in the cross-coupled pair), will sustain steady-state oscillations only at frequencies ω_0 for which:

- The loop gain is equal to unity in absolute magnitude, i.e. $\left|g_m \cdot Z(j\omega_0)^2\right| = 1$.
- The phase shift around the loop is zero or integer multiple of 2π, i.e. $\angle g_m \cdot Z(j\omega_0) = 2\pi n$, $n = 0, 1, 2, \ldots$

To fulfill the Barkhausen criteria in practice, the transconductance g_m of the transistor has to meet the condition $g_m > 2/R_p$. Under this constraint, it is easy to demonstrate that the system may oscillate at a frequency F_{osc} given by,

$$F_{osc} = \frac{\omega_0}{2\pi} = \frac{1}{2\pi\sqrt{L_{eq}C_{eq}}} \tag{1}$$

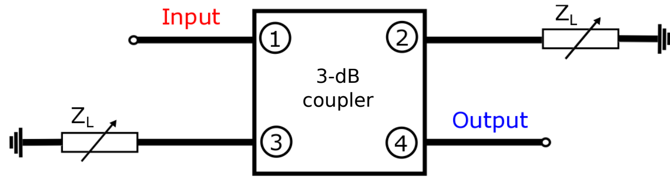

Fig. 4. General architecture of a RTPS with tunable loads. Port 1 is the input port, port 2 is the forward port, port 3 is the coupled port, and port 4 is the isolated port of the 3-dB coupler.

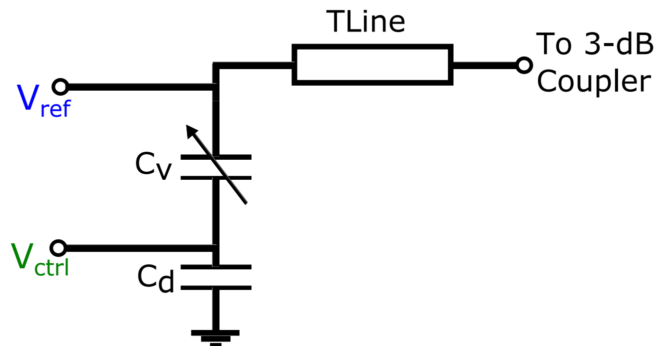

Fig. 5. Tunable loads for the considered RTPS case study.

using the same notation previously defined.

In the following, we will demonstrate that this oscillation frequency is a function of the phase shift introduced by the phase shifter during normal operation, in such a way that the measurement of the phase shift can be replaced by the measurement of F_{osc}. Let us evaluate the phase shift introduced by a RTPS. Figure 4 presents the general topology of an ideal RTPS. It is composed of an ideal 3-dB coupler and two variable loads. If we denote Γ as the reflection coefficient at ports 2 and 3, it can be demonstrated that the phase shift φ between ports 1 and 4 can be written as

$$\varphi = \pi/2 + \arg(\Gamma). \tag{2}$$

Multiple structures have been proposed to implement the loads, including switched capacitors, switched stubs, varactors, etc. In our case study we will consider varactor loads. Figure 5 shows a practical implementation of these varactor loads, which consists in a transmission line, a MOS varactor (usually implemented as an array of varactors in parallel) and one decoupling capacitor C_d. The capacitance of the varactor, C_v, is controlled by the DC voltage difference applied to its ports $(V_{ref} - V_{ctrl})$. In this configuration, equation (2) can be developed as

$$\varphi = \frac{\pi}{2} - 2\arg\left(\frac{Z_0 C_v \omega}{1 - L_c C_v \omega^2}\right) \tag{3}$$

where, in the sake of simplicity, it has been assumed that the varactors and the transmission line are ideal devices without ohmic losses, Z_0 represents the input impedance of the phase shifter, and L_c is the equivalent inductance of the transmission line.

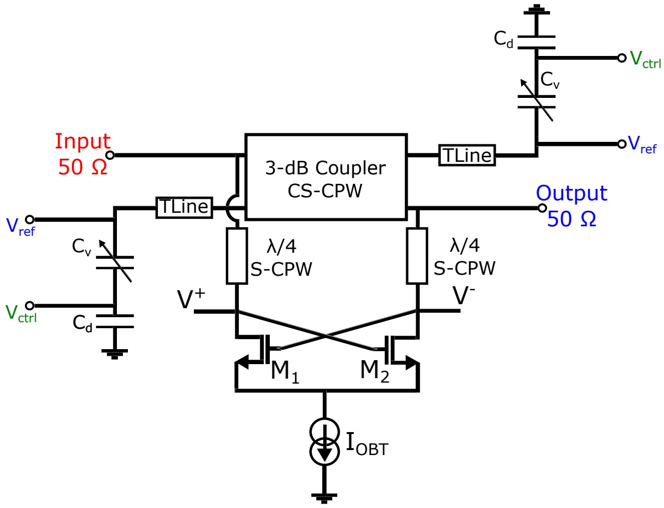

Fig. 6. Proposed RTPS with built-in OBT.

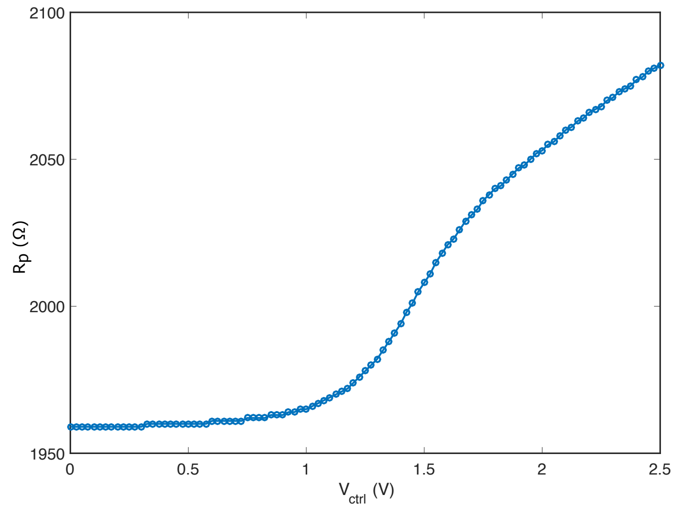

Fig. 7. Ohmic losses, R_p, in the considered reflection-type phase shifter at 60 GHz, obtained by electromagnetic simulation, as a function of the varactors bias voltage V_{ctrl}.

As it can be observed, the phase shift introduced by the phase shifter at a given frequency is a function of the varactor capacitance C_v. If we go back to the expression of the oscillation frequency in test mode given by equation (1), it is easy to see that the oscillation frequency is also a function of the varactor capacitance (being C_{eq} a function of the intrinsic impedance Z_0 and the varactor capacitance). Hence, it can be concluded that the phase shift introduced by the phase shifter in normal operation is correlated to the oscillation frequency in the proposed OBT configuration, as we intended to demonstrate. Moreover, it is interesting to notice that a similar analysis can be carried out for the amplitude of the oscillation: given that the impedance of the RTPS is a function of C_v and ω, variations in the oscillation frequency also result in variations in the oscillation amplitude.

III. Practical Implementation and Results

To validate the proposed OBT strategy, a proof-of-concept phase shifter with built-in OBT was designed in STMicroelectronics 55-nm BiCMOS technology. The selected device under test is a RTPS with varactor loads employing a 3-dB coupler based on a Coupled Slow-wave CoPlanar Waveguide architecture [19]. The selected DUT has a maximum phase shift tuning range of 55° at a central frequency of 60 GHz.

Figure 6 shows a block diagram of the DUT with added OBT circuitry. A nMOS cross-coupled pair has been co-designed together with the phase shifter in order to enable oscillations during the test mode. The cross-coupled pair is connected to the input and output nodes of the phase shifter using quarter-wavelength slow-wave CoPlanar Waveguides (CPWs) [20]. Transistors were sized in order to a) comply with the Barkhausen criteria to ensure sustained oscillation in test mode, and b) minimize the impact on the phase shifter performance during normal operation. It is important to note that in the proposed architecture no RF switches are needed to alternate between normal and OBT operation. Test mode is activated simply by turning on the current source I_{OBT} and normal operation is recovered by turning off I_{OBT}.

To meet the conditions in the Barkhausen criteria, the cross-coupled pair has to compensate the ohmic losses in the equivalent LC-tank. Thus, the equivalent negative resistor seen from the ports of the cross-coupled pair ($V+$ and $V-$ in Fig. 6), that is, $R_{neg} = -2/g_m$, where g_m is the transconductance of the transistors in the pair, has to comply with the design equation,

$$|R_{neg}| \leqslant R_p \implies g_m \geqslant \frac{R_p}{2}, \tag{4}$$

where R_p represents the ohmic losses in the phase shifter equivalent LC-tank seen from the $V+$ and $V-$ nodes. Figure 7 shows this resistance R_p as a function of the biasing voltage V_{ctrl} applied to the phase shifter, obtained by electromagnetic simulation of the system with ANSYS HFSS. Note that for this analysis, in the OBT configuration proposed in Fig. 6, the quarter-wavelength transmission lines are included in the tank, that is, the equivalent resistance is computed from the output nodes of the resulting oscillator. To comply with the Barkhausen criteria, nMOS transistors were sized to $W = 300$ μm, $L = 60$ nm, which yields a value of $|R_{neg}| = 89$ Ω when I_{OBT} is set to 6 mA.

Under the described conditions, and again according to the Barkhausen criteria, the system produces sustained oscillations at frequencies for which the total phase shift around the loop is 2π, that is, when the phase shift at the nodes of the phase shifter is π (neglecting layout parasitics). Figure 9 represents the phase shift between the nodes of the phase shifter when it is configured as an oscillator as a function of the biasing voltage V_{ctrl}, obtained by electromagnetic simulations. As it can be observed, the π phase shift can be achieved for the complete tuning range of V_{ctrl}, and the output frequencies compatible with the oscillation criteria are in the range from 14 GHz to 17 GHz.

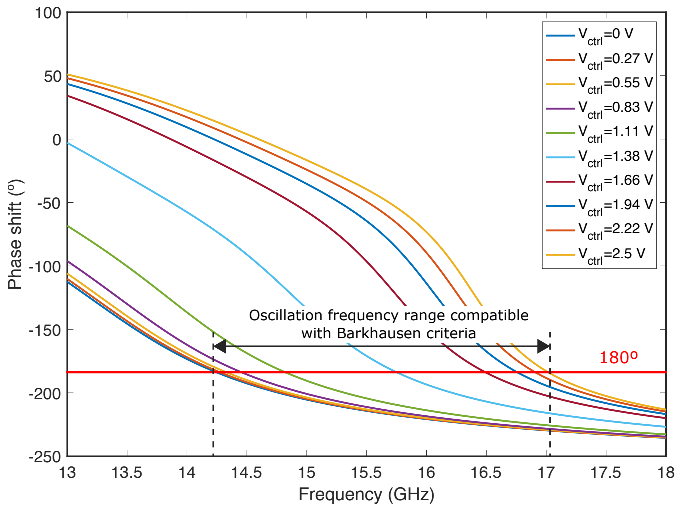

Fig. 8. Oscillation frequencies compatible with the Barkhausen criteria as a function of the bias voltage V_{ctrl}, obtained by electromagnetic simulation.

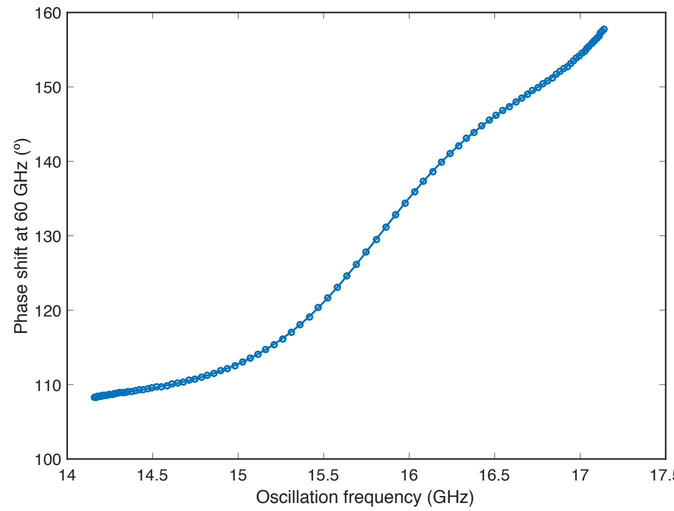

Fig. 9. Phase shift introduced by the phase shifter at 60 GHz as a function of the oscillation frequency in OBT mode.

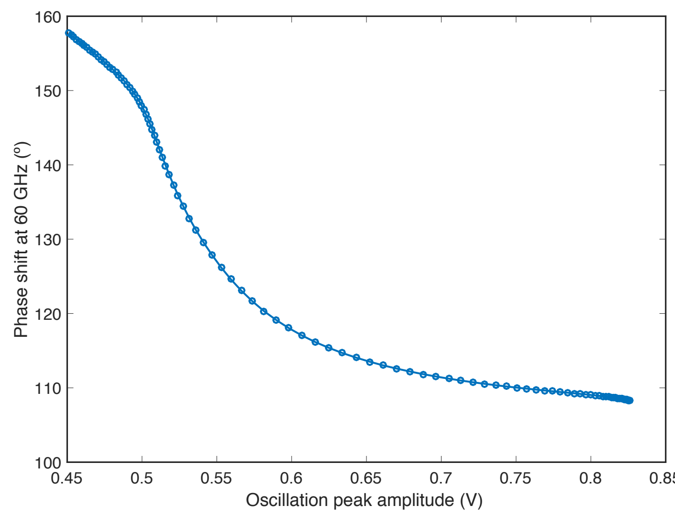

Fig. 10. Phase shift introduced by the phase shifter at 60 GHz as a function of the oscillation amplitude in OBT mode.

Regarding the impact of the added test circuitry on the performance of the original phase shifter without test circuitry, electromagnetic simulations show that the worst-case insertion loss for the original phase shifter without the OBT circuitry is of 1 dB, while the insertion loss of the phase shifter with built-in OBT during normal operation is 1.4 dB. The degradation of the insertion loss is only 0.4 dB, which is negligible for most applications. In the same line, the worst-case return loss is 28 dB for the original phase shifter, while the introduction of the OBT circuitry gives a worst-case return loss of 20 dB in normal operation mode, which still represents a good adaptation of the phase shifter.

During OBT mode, the oscillation frequency of the resulting oscillator is a signature of the phase shift introduced by the phase shifter. Figure 9 shows the phase shift introduced by the phase shifter at 60 GHz as a function of the oscillation frequency in OBT mode, obtained by electromagnetic simulation. As it can be observed, the measurement of the phase shift can be replaced by the measurement of the oscillation frequency. In addition, the amplitude of the resulting oscillation in OBT mode is another signature typically employed in classical OBT strategies [15] to complement the frequency signature. Fig. 10 shows the phase shift introduced by the phase shifter at 60 GHz as a function of the oscillation amplitude in OBT mode. As it can be observed, the measurement of the oscillation amplitude is also a simple signature that can be used to replace the complex measurement of the phase shift. The 3D plot in Fig. 11 illustrates the equivalence of the proposed measurements and represents the phase shift at 60 GHz as a function of both the oscillation frequency and amplitude in OBT mode. In other words, it is shown that we can replace the measurement of phase shift at 60 GHz by measurements of frequency and/or amplitude in the frequency range of 14 GHz to 17 GHz.

These results show that applying OBT to mm-wave phase shifters is not only a feasible test approach, but it opens the door to simple on-chip characterization of phase shifters with reduced hardware resources. Future work will include the extension of the proposed OBT architecture to integrate on-chip amplitude and/or frequency detectors that may enable on-chip self-test and calibration applications. Moreover, it is particularly interesting to consider the extension of the proposed technique to complete phased arrays. Phase shift differences between the different branches of a phased array will appear as differences in the oscillation frequency and amplitude in OBT mode. Measuring frequency and amplitude differences is a much simpler and precise task than measuring phase differences, which opens the door to future BIST applications for phased arrays based on the proposed OBT strategy.

IV. Conclusions

In this paper, it has been shown for the first time that an Oscillation-Based Test technique could be suitable for the

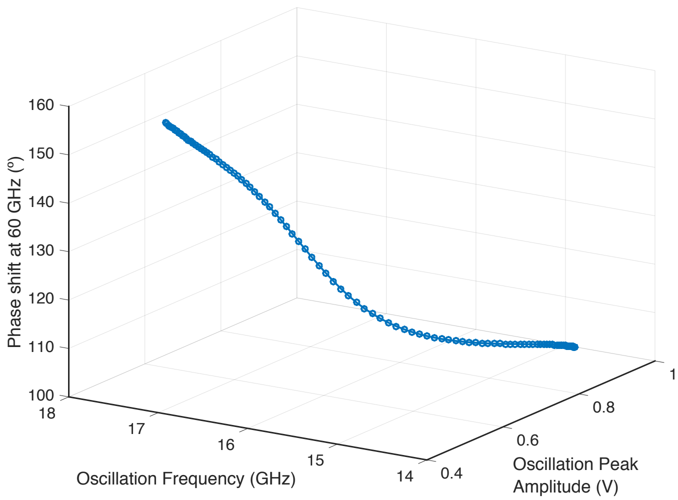

Fig. 11. Phase shift introduced by the phase shifter at 60 GHz as a function of both the oscillation frequency and amplitude in OBT mode.

characterization of integrated mm-wave phase shifters. The proposed OBT technique is based in the reconfiguration of the phase shifter under test as an oscillator during test mode and it enables the replacement of complex phase shift measurements at high frequencies by simpler signatures such as the frequency and amplitude of the resulting oscillator.

The fundamentals of the proposed test strategy have been analytically explored, and the proposed technique has been validated in a proof-of-concept prototype designed in STMicroelectronics 55-nm BiCMOS technology. The designed prototype consists in a reflection-type phase shifter with varactor loads with a built-in nMOS cross-coupled pair to enable oscillations during OBT mode. Electromagnetic and electrical simulations show the feasibility of the proposed technique with a negligible impact on the performance of the phase shifter during normal operation. The proposed OBT technique requires very few hardware resources and may be a promising solution for practical BIST applications of phased arrays.

Acknowledgements

This work has been partially funded by the TARANTO project.

References

[1] A. Hajimiri, H. Hashemi, A. Natarajan, X. Guan, and A. Komijani, "Integrated Phased Array Systems in Silicon," *Proceedings of the IEEE*, vol. 93, pp. 1637–1655, Sept 2005.

[2] W. Roh, J. Y. Seol, J. Park, B. Lee, J. Lee, Y. Kim, J. Cho, K. Cheun, and F. Aryanfar, "Millimeter-wave beamforming as an enabling technology for 5G cellular communications: theoretical feasibility and prototype results," *IEEE Communications Magazine*, vol. 52, pp. 106–113, February 2014.

[3] J. Bae, Y. S. Choi, J. S. Kim, and M. Y. Chung, "Architecture and performance evaluation of mmwave based 5g mobile communication system," in *2014 International Conference on Information and Communication Technology Convergence (ICTC)*, pp. 847–851, Oct 2014.

[4] J. W. Jeong, J. Kitchen, and S. Ozev, "A self-compensating built-in self-test solution for RF phased array mismatch," in *2015 IEEE International Test Conference (ITC)*, pp. 1–9, Oct 2015.

[5] C. Y. Kim, D. W. Kang, and G. M. Rebeiz, "A 44-46-GHz 16-Element SiGe BiCMOS High-Linearity Transmit/Receive Phased Array," *IEEE Transactions on Microwave Theory and Techniques*, vol. 60, pp. 730–742, March 2012.

[6] M. Shafiee and S. Ozev, "Contact-less near-field measurement of RF phased array antenna mismatches," in *2017 22nd IEEE European Test Symposium (ETS)*, pp. 1–6, May 2017.

[7] X. Guan, H. Hashemi, and A. Hajimiri, "A fully integrated 24-GHz eight-element phased-array receiver in silicon," *IEEE Journal of Solid-State Circuits*, vol. 39, pp. 2311–2320, Dec 2004.

[8] S. Jeon, Y. J. Wang, H. Wang, F. Bohn, A. Natarajan, A. Babakhani, and A. Hajimiri, "A Scalable 6-to-18 GHz Concurrent Dual-Band Quad-Beam Phased-Array Receiver in CMOS," *IEEE Journal of Solid-State Circuits*, vol. 43, pp. 2660–2673, Dec 2008.

[9] S. Y. Kim, O. Inac, C. Y. Kim, D. Shin, and G. M. Rebeiz, "A 76-84-GHz 16-Element Phased-Array Receiver With a Chip-Level Built-In Self-Test System," *IEEE Transactions on Microwave Theory and Techniques*, vol. 61, pp. 3083–3098, Aug 2013.

[10] O. Inac, F. Golcuk, T. Kanar, and G. M. Rebeiz, "A 90-100-GHz Phased-Array Transmit/Receive Silicon RFIC Module With Built-In Self-Test," *IEEE Transactions on Microwave Theory and Techniques*, vol. 61, pp. 3774–3782, Oct 2013.

[11] T. Kanar and G. M. Rebeiz, "A 2-15 GHz built-in-self-test system for wide-band phased arrays using self-correcting 8-state I/Q mixers," in *2016 IEEE MTT-S International Microwave Symposium (IMS)*, pp. 1–4, May 2016.

[12] K. Greene, V. Chauhan, and B. Floyd, "Code-modulated embedded test for phased arrays," in *2016 IEEE 34th VLSI Test Symposium (VTS)*, pp. 1–4, April 2016.

[13] K. Arabi and B. Kaminska, "Oscillation-test strategy for analog and mixed-signal integrated circuits," in *Proceedings of 14th VLSI Test Symposium*, pp. 476–482, Apr 1996.

[14] K. Arabi and B. Kaminska, "Efficient and accurate testing of analog-to-digital converters using oscillation-test method," *Proceedings European Design and Test Conference. ED & TC 97*, pp. 348–352, 1997.

[15] G. Huertas, D. Vazquez, E. J. Peralias, A. Rueda, and J. L. Huertas, "Practical oscillation-based test of integrated filters," *IEEE Design Test of Computers*, vol. 19, pp. 64–72, Nov 2002.

[16] G. Huertas, D. Vazquez, A. Rueda, and J. L. Huertas, "Built-in self-test in mixed-signal ICs: a DTMF macrocell," *VLSI Design 2000. Wireless and Digital Imaging in the Millennium. Proceedings of 13th International Conference on VLSI Design*, pp. 568–571, 2000.

[17] B. T. Henoch and P. Tamm, "A 360° Reflection-Type Diode Phase Modulator (Correspondence)," *IEEE Transactions on Microwave Theory and Techniques*, vol. 19, no. 1, pp. 103–105, 1971.

[18] B. Razavi, *RF Microelectronics (2Nd Edition)*. Upper Saddle River, NJ, USA: Prentice Hall Press, 2nd ed., 2011.

[19] Z. Iskandar, J. Lugo-Alvarez, A. Bautista, E. Pistono, F. Podevin, V. Puyal, A. Siligaris, and P. Ferrari, "A 30-50 GHz reflection-type phase shifter based on slow-wave coupled lines in BiCMOS 55 nm technology," *2016 46th European Microwave Conference (EuMC)*, pp. 1413–1416, 2016.

[20] A. Bautista, A. L. Franc, and P. Ferrari, "Accurate Parametric Electrical Model for Slow-Wave CPW and Application to Circuits Design," *IEEE Transactions on Microwave Theory and Techniques*, vol. 63, no. 12, pp. 4225–4235, 2015.